Research Square

Preprints are preliminary reports that have not undergone peer review.
They should not be considered conclusive, used to inform clinical practice,
or referenced by the media as validated information.

Gestational age-specific reference intervals for maternal ophthalmic artery Doppler indices at 28–32 weeks of gestation

Mina Ataei
Alborz University of Medical Sciences
Mansoureh Yazdkhasti
Mansoyazd@yahoo.com
Alborz University of Medical Sciences
Zahra Sadat Khonsarian
Alborz University of Medical Sciences
Maryam Panahi
Alborz University of Medical Sciences
Maryam Babazadeh
Alborz University of Medical Sciences
Sara Esmaelzadeh Saeieh
Alborz University of Medical Sciences
Masoumeh Saleh
Tehran University of Medical Sciences
Mahmood Bakhtiyari
Alborz University of Medical Sciences

Research Article

Keywords: Ophthalmic Arteries, ultrasonography, Pregnancy, Pre-Eclampsia, Gestational Age

Posted Date: November 17th, 2026

DOI: https://doi.org/10.21203/rs.3.rs-11322445/v1

License: This work is licensed under a Creative Commons Attribution 4.0 International License.
Read Full License

Additional Declarations: No competing interests reported.

Gestational age-specific reference intervals for maternal ophthalmic artery Doppler indices at 28–32 weeks of gestation

Mina Ataei[1], Mansoureh Yazdkhasti[2*], Zahra Sadat Khonsarian[1], Maryam Panahi[1], Maryam Babazadeh[3*], Sara Esmaelzadeh Saeieh[2], Masoumeh Saleh[4], Mahmood Bakhtiyari[5]

1. Department of Obstetrics and Gynecology, School of Medicine, Alborz University of Medical Sciences, Karaj, Iran
2. *Department of Reproductive Health, Social Determinants of Health Research Center, Alborz University of Medical Sciences, Karaj, Iran
3. *Department of Community Medicine, Alborz University of Medical Sciences, Karaj, Iran
4. Department of Obstetrics and Gynecology, Shariati Hospital, Tehran University of Medical Sciences, Tehran, Iran
5. Non-Communicable Diseases Research Center, Alborz University of Medical Sciences, Karaj, Iran

*Corresponding authors: Mansoureh Yazdkhasti (PhD), Maryam Babazadeh (MD)

Postal address: Hasan Abad Blvd,ooge St, Karaj, Iran Postal code/ P.O. Box: 3149779453

Telephone number: +98 026-32563328

Fax Number: +98 32556655

Email Address: Mansoyazd@yahoo.com

ORCID: https://orcid.org/0000-0002-9298-4531

Email Address: drbabazadeh525@gmail.com

ORCID: https://orcid.org/9007-4551-0003-0000

Abstract

Background and Objective: Preeclampsia is associated with impaired maternal vascular adaptation and altered cerebral circulatory resistance. The ophthalmic artery, owing to its non-invasive accessibility and shared origin with the intracranial circulation, offers a window into these changes; however, interpretation of its Doppler indices requires reference values appropriate to the population and gestational age under study. This study aimed to establish reference values for maternal ophthalmic artery Doppler indices at 28 to 32 weeks of gestation.

Methods: In this historical cohort study, data from 386 pregnant women with complete bilateral ophthalmic artery Doppler measurements were analyzed. The primary reference population comprised 342 pregnancies that did not develop preeclampsia during follow-up. Location–scale models were fitted for first peak systolic velocity (PSV1), second peak systolic velocity (PSV2), pulsatility index (PI), and the PSV2/PSV1 ratio, separately for the right eye, left eye, and bilateral mean. Identity, square-root, and logarithmic transformations, together with alternative functions of gestational age, were compared using the corrected Akaike information criterion (AICc). The 2.5th and 97.5th percentiles defined the central 95% reference interval, and 90% confidence intervals for these limits were obtained from 1,000 bootstrap resamples.

Results: Of the 386 participants, 44 (11.4%) subsequently developed preeclampsia. In the reference population, the model-based median bilateral mean PSV1 was 32.01 cm/s, with the reference interval narrowing from 11.93–52.08 cm/s at week 28 to 16.59–47.43 cm/s at week 32. The median PSV2 was 16.89 cm/s, with a reference interval of 7.94–29.17 cm/s that remained constant across the study interval. Bilateral mean PI (median, 1.996; reference interval, 1.144–3.085) and the peak ratio (median, 53.65%; reference interval, 37.24%–77.29%) were likewise stable across this interval. Lin's concordance correlation coefficients for PSV1, PSV2, PI, and the peak ratio were 0.960, 0.997, 0.993, and 0.983, respectively. In adjusted analysis, each 1-SD increase in the peak ratio was associated with higher odds of subsequent preeclampsia (OR, 8.60; 95% CI, 5.09–14.51) and showed the highest apparent discriminative performance (AUC, 0.940; 95% CI, 0.883–0.997).

Conclusion: This study provides model-based reference intervals for four principal maternal ophthalmic artery Doppler indices at 28 to 32 weeks of gestation. The medians of PSV1, PSV2, PI, and the peak ratio remained stable across this interval; only the dispersion of PSV1 narrowed as gestational age advanced. The high degree of interocular agreement supports the use of the bilateral mean in research settings. The strong associations of the peak ratio and PI with subsequent preeclampsia support their biological relevance; however, predictive estimates require independent external validation before clinical application.

Keywords: Ophthalmic Arteries, ultrasonography, Pregnancy, Pre-Eclampsia, Gestational Age

Introduction

Pregnancy is accompanied by extensive cardiovascular adaptations, including increased blood volume and cardiac output, decreased systemic vascular resistance, and reorganized regulation of blood flow to preserve perfusion of vital organs (1). These adaptations are particularly important in the cerebral circulation, where the margin of vascular safety is narrow, and dysregulation can manifest as headache, visual disturbances, seizures, and end-organ damage (2,3).

The ophthalmic artery is a branch of the internal carotid artery and, owing to its ready accessibility through the closed eyelid, provides an indirect window into orbital vascular resistance and the intracranial circulation (4–6). Its Doppler waveform typically displays two systolic peaks: a first peak (PSV1) and a second peak (PSV2), from which the pulsatility index and the PSV2-to-PSV1 ratio can also be derived (7). Physiological and reference studies have shown that some of these indices change over the course of pregnancy, whereas others remain relatively stable (8–11).

Preeclampsia is a multisystem, pregnancy-specific disorder characterized by new-onset hypertension with evidence of end-organ involvement after mid-pregnancy (1,12). Its pathophysiology involves an interplay of placental dysfunction, an imbalance of angiogenic factors, endothelial activation, inflammation, and dysregulated maternal vascular regulation (13–17). Decreased resistance and increased flow in the orbital vessels—manifested by elevated PSV2 and peak ratio together with reduced PI—have been proposed as markers of cerebral hyperperfusion in the maternal circulation (18).

Although a substantial portion of the literature has focused on the prediction or diagnosis of preeclampsia, interpretation of an abnormal index first requires knowledge of its distribution in low-risk, normotensive pregnancies. A reference interval is the range encompassing the central portion of an index's distribution in a reference population, conventionally defined by the 2.5th and 97.5th percentiles. For variables that depend on gestational age, applying a single fixed interval risks conflating physiological variation with disease; continuous or week-specific modeling is therefore essential (10).

Reference studies from different countries have reported discrepant trends for PI, RI, PSV, and the peak ratio. Some have described a decline in PI and RI with advancing gestational age, whereas others have reported relative stability of the peak ratio or even nonlinear patterns (7–9). Differences in population composition, equipment, angle of insonation, number of measurements per eye, and statistical approach may all contribute to this heterogeneity. Establishing local reference data, accompanied by rigorous methodological reporting and assessment of inter -ocular agreement, is therefore important (10).

In Iran, research use of ophthalmic artery Doppler in pregnancy has grown; however, reference values specific to weeks 28–32, derived from a reasonably large population with bilateral measurements and a flexible statistical model, remain limited. This gestational window is of particular clinical relevance because a subset of preeclampsia cases becomes clinically apparent

shortly after such an assessment, while third-trimester hemodynamic changes may simultaneously influence the distribution of these indices (13–18).

In the absence of validated reference intervals, an unusually high or low value may be interpreted solely in relation to thresholds derived from a prediction study or an external population. Such an approach carries two risks: first, mislabeling physiological variation as a pathological state; and second, overlooking a genuine deviation because the applied reference limits are poorly matched to the gestational age or population under study. Recent work has likewise emphasized the need for local validation and technique standardization (11).

A further methodological consideration concerns the distributional characteristics of Doppler indices. The peak ratio and PI can exhibit skewness or heavy tails, and the dispersion of PSV may change with gestational age. Consequently, computing the mean ± 1.96 SD without examining transformation, the location function, heteroscedasticity, and residual diagnostics risks producing inappropriate reference limits. A six-step location–scale approach with GAMLSS sensitivity analysis allows the location, scale, and, where necessary, shape of the distribution to be evaluated transparently (19,20).

The central research question, therefore, was to determine the central 95% reference limits for PSV1, PSV2, PI, and the PSV2/PSV1 ratio in the right eye, left eye, and bilateral mean at 28 to 32 completed weeks of gestation, and to determine whether these limits change with gestational age. In addition, interocular agreement and the potential biological relevance of these indices in relation to subsequent preeclampsia were examined as supplementary analyses.

Methods

Study Design and Setting

The participants of the current study included pregnant women who attended routine prenatal visits between 2020 and 2025. Both hospitals are tertiary referral centers providing specialized care for high-risk pregnancies. Pregnant women with maternal or fetal complications are routinely referred to these centers for specialized assessment and management.

Participants and Eligibility Criteria

The study population comprised 386 eligible pregnant women. Women were eligible if they had a singleton pregnancy and a gestational age of 28–32 weeks at the time of ophthalmic artery Doppler assessment. Women with chronic hypertension, a history of preeclampsia, type 1 or type 2 diabetes mellitus, autoimmune or vascular disease, chromosomal abnormalities, or major fetal anomalies were excluded.

Participants were subsequently classified according to pregnancy outcome. The reference population comprised women who remained free of preeclampsia throughout follow-up, whereas the preeclampsia group comprised women who subsequently developed preeclampsia.

The reference population was used to establish the physiological distribution of ophthalmic artery Doppler indices. Participants who subsequently developed preeclampsia were excluded from the

reference population to minimize the potential influence of the preclinical phenotype of preeclampsia on estimates of physiological reference values. All 386 participants were retained for cohort description, right–left agreement analyses, and analyses evaluating the association between ophthalmic artery Doppler indices and subsequent preeclampsia.

Sampling and Sample Size

Eligible participants were selected using simple random sampling from the available sampling frame [https://randomset.ir/Home/RandomNumberGenerator].

All 386 participants included in the final analysis had complete measurements of the primary ophthalmic artery Doppler indices for both eyes at 28–32 weeks of gestation. Of these, 342 women remained free of preeclampsia throughout follow-up and constituted the reference population, while 44 women developed preeclampsia during follow-up.

Among women in the reference population, the numbers assessed at 28, 29, 30, 31, and 32 weeks of gestation were 67, 72, 53, 76, and 74, respectively.

Data Collection

Maternal variables included maternal age, body mass index (BMI), interpregnancy interval, ethnicity, medical and medication history, family history of preeclampsia, mode of conception, and delivery status. Pregnancy- and fetal-related variables included gestational age at Doppler assessment, fetal abdominal circumference percentile, estimated fetal weight percentile, amniotic fluid status, mean uterine artery pulsatility index (PI), pregnancy-associated plasma protein-A (PAPP-A) expressed as multiples of the median (MoM), gestational age at delivery, and birth weight.

Gestational age was determined using standardized obstetric ultrasonographic dating. Fetal abdominal circumference and estimated fetal weight percentiles were recorded as measures of fetal growth, while the mean uterine artery PI was recorded to characterize the uteroplacental circulation. PAPP-A values were obtained from first-trimester screening records. The occurrence, severity, and gestational age at onset of preeclampsia were determined from follow-up records.

Ophthalmic Artery Doppler Protocol: Ophthalmic artery Doppler examinations were performed using a 7–15 MHz linear-array transducer. Participants were examined in the supine position, and the transducer was placed horizontally over the closed eyelid using adequate acoustic gel and minimal pressure. The ophthalmic artery was identified using color Doppler, and the insonation angle was maintained below 20°. For each eye, three to five consecutive stable cardiac cycles were recorded. Peak systolic velocity 1 (PSV1), peak systolic velocity 2 (PSV2), and pulsatility index (PI) were obtained from the spectral Doppler waveform. PSV1 was defined as the first systolic peak, and PSV2 as the second systolic peak of the ophthalmic artery waveform. The peak ratio (PR) for each eye was calculated as:

$$PR = 100 \times (PSV2/PSV1)$$

For each Doppler index, the bilateral mean was calculated as the arithmetic mean of the corresponding measurements obtained from the right and left eyes.

To ensure consistency and reproducibility, PR values were recalculated directly from the recorded PSV1 and PSV2 measurements rather than relying on previously derived ratio values. Raw Doppler variables were retained in the dataset, while derived analytical variables were generated separately.

Non-positive PAPP-A values were considered invalid and coded as missing before analysis. Maternal age values outside the prespecified range of 15–55 years were excluded only from analyses requiring maternal age [this criterion should be retained only if it was prespecified and actually applied].

Data structure and analytical populations

The full analytical cohort comprised pregnant participants assessed at 28–32 completed weeks of gestation. Because the primary objective was to define physiological reference values, pregnancies that remained free of preeclampsia throughout follow-up formed the primary reference cohort. The full cohort was retained for secondary, exploratory analyses of subsequent preeclampsia.

Variable derivation and quality control

Birth weight and fetal-percentile fields were harmonized to grams and percentage points, respectively, using prespecified scale checks while retaining the original fields. Nonpositive pregnancy-associated plasma protein-A (PAPP-A) multiples of the median were retained in the source variable and set to missing in the analysis variable. The ophthalmic artery second-to-first peak systolic velocity ratio was recalculated separately on each side as 100 × PSV2/PSV1; the bilateral mean ratio was the arithmetic mean of the two recalculated side-specific ratios. Recalculated ratios were used in all inferential analyses because the stored ratio fields showed material discrepancies. Maternal ages outside the prespecified 15–55-year plausibility interval were set to missing only in the analysis-safe age variable used for covariate adjustment. Chronology and biological-consistency checks were retained as explicit quality-control flags. No single imputation was performed; each analysis used all observations with the required variables available.

Descriptive and group-comparison analyses

Continuous variables were summarized using the number of available observations, missingness, mean and standard deviation, median and interquartile range, range, selected type-8 empirical percentiles, skewness, and excess kurtosis. Categorical variables were summarized as counts and percentages. Summaries were produced overall, by completed gestational week at Doppler assessment, and by subsequent preeclampsia status. Exploratory continuous-variable comparisons combined Welch t tests, Wilcoxon rank-sum tests, and standardized mean differences. Categorical variables were compared using Pearson χ^2 or Fisher exact tests according to expected cell

frequencies. Benjamini–Hochberg false-discovery-rate adjustment was applied within each prespecified family of related comparisons.

Reference-interval estimation

Gestational-age-specific reference intervals were estimated separately for right-sided, left-sided, and bilateral-mean PSV1, PSV2, pulsatility index (PI), and PSV2-to-PSV1 ratio. The protocol-concordant primary analysis used a transformation-aware location–scale framework. Identity, square-root, and logarithmic transformations were compared using residual skewness and kurtosis, with preference for the least complex transformation when diagnostic performance was similar. Candidate location functions comprised constant, linear, quadratic, cubic, natural cubic spline, and first-degree fractional-polynomial functions of completed gestational age. Models were ranked using the small-sample corrected Akaike information criterion (AICc); when candidate models were within 2 AICc units, the less complex specification was selected. Conditional scale was estimated by regressing scaled absolute residuals—absolute residual multiplied by $\sqrt{(\pi/2)}$—on gestational age using constant, linear, and quadratic functions. Model z scores were calculated as transformed residuals divided by the fitted conditional standard deviation. After inverse transformation, the 2.5th and 97.5th conditional percentiles defined the central 95% reference interval. At completed weeks 28–32, 90% confidence intervals for the lower limit, median, and upper limit were estimated from 1,000 participant-level bootstrap resamples.

Model diagnostics and sensitivity analyses

Model adequacy was evaluated using standardized-residual plots across gestational age, normal Q–Q plots, z-score moments, normality tests, heteroscedasticity tests when estimable, observed central-95% coverage, and statistical-outlier counts. An observation with $|z| > 4$ was classified as a model outlier; such observations remained in the primary analysis and were excluded only in a separate sensitivity analysis. Type-8 empirical 2.5th, 50th, and 97.5th percentiles were also calculated overall and within each completed-week partition. Partitions with fewer than 120 observations were explicitly flagged, and model-based intervals were retained as the primary week-specific estimates. Additional sensitivity analyses used the complete screened cohort and generalized additive models for location, scale and shape, comparing normal, log-normal, and Box–Cox Cole–Green distributional families by Akaike information criterion. These analyses were considered diagnostic and did not replace the prespecified primary model.

Bilateral agreement

Right–left agreement was assessed using the paired mean difference (right minus left) with its 95% confidence interval, Bland–Altman 95% limits of agreement, Pearson and Spearman correlations, Lin concordance correlation coefficient, paired t tests, and paired Wilcoxon signed-rank tests. False-discovery-rate-adjusted P values were reported for the paired comparisons.

Secondary preeclampsia analyses

Preeclampsia analyses were prespecified as secondary and exploratory. Separate logistic regression models estimated the odds ratio for subsequent preeclampsia per 1-standard-deviation increase in each Doppler endpoint. Adjusted models included completed gestational week at Doppler assessment, analysis-safe maternal age, and maternal body mass index. Bilateral mean indices were additionally evaluated using receiver-operating-characteristic curves with DeLong 95% confidence intervals. Sensitivity and specificity were summarized at the within-sample Youden-optimal threshold. Because these thresholds were derived and evaluated in the same cohort, they were treated as apparent-performance summaries rather than clinical decision limits. Severe and early-onset preeclampsia subgroups were described without multivariable subgroup modeling because of sparse events.

Statistical conventions and software

All tests were two-sided. Effect estimates are presented with 95% confidence intervals unless otherwise specified; bootstrap confidence intervals for reference limits are 90%. Multiplicity-adjusted results are identified as false-discovery-rate P values. Analyses were performed in R version 4.5.0 with a prespecified random seed (20260726), and figures were exported at 600 dpi. The preeclampsia analyses were interpreted as hypothesis-generating and were not used to alter the primary reference population or reference-limit estimation.

Results

Cohort assembly and analytical populations

The final analytical cohort comprised 386 participants assessed at 28–32 completed weeks, all with complete bilateral measurements for the 12 primary ophthalmic artery Doppler endpoints (Figure 1). Forty-four pregnancies developed preeclampsia during follow-up (11.4%), leaving 342 participants in the primary reference cohort. The primary cohort included 67, 72, 53, 76, and 74 participants at completed weeks 28, 29, 30, 31, and 32, respectively. Among the 44 cases, 38 (86.4%) were mild and 6 (13.6%) were severe; 7 (15.9%) were early-onset and 37 (84.1%) were late-onset. The analytical handling of prespecified data-quality findings is summarized in Supplementary Table S1.

Data-quality findings

Stored and recalculated PSV2-to-PSV1 ratios differed by more than 0.5 percentage points in 13 right-sided records (3.4%) and 87 left-sided records (22.5%); the maximum absolute discrepancies were 59.81 and 69.74 percentage points, respectively. Consequently, all ratio analyses used the recalculated fields (Supplementary Figure S1). Nine nonpositive PAPP-A MoM values were set

to missing in the analysis variable. Two maternal ages outside 15–55 years were omitted only from age-adjusted models, yielding 384 participants and 44 events in those models. Three records had delivery gestational age below Doppler gestational age; delivery timing was not an input to the primary reference-interval or Doppler–preeclampsia models, and the source values remained unchanged.

Participant characteristics

Participants who subsequently developed preeclampsia were older (median, 32 [IQR, 29–36] vs 30 [26–34] years; FDR P=0.021), had higher body mass index (27.3 [23.7–30.0] vs 25.0 [22.4–28.3] kg/m²; FDR P=0.011), and were assessed later in gestation (31 [30.4–32] vs 30 [29–31] completed weeks; FDR P<0.001) (Table 1). They also had lower fetal abdominal circumference and estimated fetal weight percentiles, higher mean uterine artery PI, and lower PAPP-A MoM (all FDR P<0.001). Mean bilateral PSV1 and PI were lower in the preeclampsia group, whereas mean bilateral PSV2 and the PSV2-to-PSV1 ratio were higher. The largest standardized mean difference was observed for the mean peak ratio (2.62), followed by mean uterine artery PI (1.89) and mean ophthalmic artery PI (−1.16). Conception method, amniotic-fluid status, and uterine artery PI category differed after multiplicity adjustment, whereas ethnicity, parity/previous-preeclampsia category, medical history, medication history, and family history did not. Overall continuous and categorical summaries are provided in Supplementary Tables S2 and S3.

Reference intervals for bilateral mean indices

All 342 participants in the primary reference cohort contributed to each Doppler endpoint. For bilateral mean PSV1, the selected identity-scale location model was constant, whereas conditional scale decreased linearly across gestation. The fitted median was 32.01 cm/s, and the central 95% reference interval narrowed from 11.93–52.08 cm/s at week 28 to 16.59–47.43 cm/s at week 32. Bilateral mean PSV2 was modeled on the square-root scale with constant location and scale; its fitted median was 16.89 cm/s and its central 95% interval was 7.94–29.17 cm/s throughout weeks 28–32. Bilateral mean PI likewise had constant square-root-scale location and scale, corresponding to a median of 1.996 and a central interval of 1.144–3.085. The bilateral mean peak ratio had constant log-scale location and scale, with a median of 53.65% and a central interval of 37.24%–77.29% (Table 2 and Figure 2). All 1,000 bootstrap resamples were successful for every endpoint and completed week. Full week-specific descriptive summaries, preeclampsia-stratified summaries, and side-specific and bilateral model-based intervals are reported in Supplementary Tables S4–S6.

Reference-model diagnostics and sensitivity analyses

Observed central-95% coverage was 93.6% for bilateral mean PSV1, 91.5% for mean PSV2, 89.8% for mean PI, and 92.1% for the mean peak ratio. Corresponding z-score standard deviations were 1.018, 1.063, 1.176, and 1.083. Mean PI and the mean peak ratio showed the most pronounced heavy-tail behavior, with excess kurtosis of 2.21 and 2.81, respectively. No |z|>4

outliers occurred for the two bilateral velocity endpoints; two occurred for mean PI and one for the mean peak ratio. Excluding these observations did not materially resolve the undercoverage of the PI or ratio models. GAMLSS model selection favored Box–Cox Cole–Green specifications for the bilateral mean PSV1, PSV2, and PI endpoints and a log-normal specification for the bilateral mean peak ratio. Accordingly, the primary limits should be interpreted as protocol-concordant model-based estimates rather than as uniformly calibrated distribution-free limits, particularly for PI and the peak ratio. Complete primary diagnostics, empirical percentiles, and GAMLSS candidate-family comparisons are reported in Supplementary Tables S7–S9. Right–left agreement

Right and left measurements showed high concordance. Lin concordance correlation coefficients were 0.960 for PSV1, 0.997 for PSV2, 0.993 for PI, and 0.983 for the peak ratio (Table 3). Mean right-minus-left biases were −0.023 cm/s for PSV1, −0.019 cm/s for PSV2, −0.004 for PI, and 0.144 percentage points for the peak ratio; all paired t-test FDR P values were at least 0.544. Bland–Altman limits of agreement were −5.29 to 5.25 cm/s for PSV1, −0.92 to 0.88 cm/s for PSV2, −0.149 to 0.142 for PI, and −5.51 to 5.79 percentage points for the peak ratio. Rank-based paired tests identified small distributional asymmetries for PSV1 and PI, but the absolute mean biases were negligible relative to between-participant variability. Complete agreement statistics and graphical assessments are provided in Supplementary Table S10.

All 12 right-sided, left-sided, and bilateral mean Doppler endpoints differed between preeclampsia and non-preeclampsia groups after false-discovery-rate correction (Supplementary Table S11). In adjusted models, each 1-SD higher bilateral mean PSV1 was associated with lower odds of subsequent preeclampsia (odds ratio [OR], 0.438; 95% CI, 0.300–0.640), whereas each 1-SD higher mean PSV2 was associated with higher odds (OR, 1.891; 95% CI, 1.360–2.630). Each 1-SD higher mean PI was associated with lower odds (OR, 0.201; 95% CI, 0.123–0.330), and each 1-SD higher mean peak ratio was associated with substantially higher odds (OR, 8.595; 95% CI, 5.092–14.508); all adjusted FDR P values were <0.001 (Table 4, panel A; Figure 3). Complete unadjusted and adjusted models are reported in Supplementary Table S12.

Exploratory discrimination and preeclampsia subtypes

Among the four bilateral mean indices, the peak ratio had the highest apparent discrimination for subsequent preeclampsia (area under the curve [AUC], 0.940; 95% CI, 0.883–0.997), followed by mean PI (AUC, 0.832; 95% CI, 0.756–0.907), mean PSV1 (AUC, 0.719; 95% CI, 0.633–0.805), and mean PSV2 (AUC, 0.678; 95% CI, 0.585–0.771) (Table 4, panel B; Figure 4). The within-sample Youden threshold for the mean peak ratio was ≥71.83%, corresponding to 93.2% sensitivity and 94.4% specificity. These values are apparent-performance estimates from the derivation cohort and are not proposed as clinical thresholds. Detailed ROC results and descriptive severity/onset summaries are reported in Supplementary Table S13. The interval from Doppler assessment to diagnosis was a median of 2 [IQR, 2–3] days among early-onset cases and 4 [3–5] days among late-onset cases; the latter distribution was strongly right-skewed.

Table 1. Participant characteristics according to subsequent preeclampsia status

Characteristic	No PE	PE	SMD	FDR P
Maternal age, years (n=340/44)	30.0 [26.0–34.0]	32.0 [29.0–36.0]	0.35	0.021
Maternal body mass index, kg/m² (n=342/44)	24.9 [22.4–28.3]	27.3 [23.7–30.0]	0.37	0.011
Gestational age at Doppler assessment, completed weeks (n=342/44)	30.0 [29.0–31.0]	31.0 [30.4–32.0]	0.63	<0.001
Fetal abdominal circumference percentile (n=342/44)	40.0 [34.0–52.1]	20.0 [2.8–45.8]	-0.49	<0.001
Estimated fetal weight percentile (n=342/44)	45.0 [30.9–58.0]	17.0 [2.0–50.0]	-0.81	<0.001
Mean uterine artery PI (n=339/44)	0.80 [0.70–0.90]	1.30 [1.10–1.70]	1.89	<0.001
PAPP-A, MoM (n=308/40)	1.15 [0.82–1.41]	0.55 [0.25–0.70]	-0.93	<0.001
Mean bilateral PSV1, cm/s (n=342/44)	31.75 [26.25–38.21]	24.35 [20.33–27.45]	-0.74	<0.001
Mean bilateral PSV2, cm/s (n=342/44)	17.00 [14.10–20.45]	21.20 [17.69–26.80]	0.68	<0.001
Mean bilateral PI (n=342/44)	1.985 [1.790–2.250]	1.280 [0.960–1.584]	-1.16	<0.001
Mean bilateral PSV2-to-PSV1 ratio, % (n=342/44)	53.56 [48.34–60.20]	90.50 [80.50–97.86]	2.62	<0.001
Iranian ethnicity	335 (98.0%)	43 (97.7%)	—	1.000
Nulliparous	171 (50.0%)	22 (50.0%)	—	0.402
Any medical history	120 (35.1%)	20 (45.5%)	—	0.381
Any medication history	105 (30.7%)	20 (45.5%)	—	0.145
Family history of preeclampsia	8 (2.3%)	1 (2.3%)	—	1.000
Spontaneous conception	308 (90.1%)	35 (79.5%)	—	0.009
In vitro fertilization	27 (7.9%)	3 (6.8%)	—	
Ovulation-induction medication	7 (2.0%)	6 (13.6%)	—	
Normal amniotic fluid	319 (93.3%)	36 (81.8%)	—	0.009
Oligohydramnios	8 (2.3%)	6 (13.6%)	—	
Polyhydramnios	14 (4.1%)	2 (4.5%)	—	
Abnormal uterine artery PI	57 (16.7%)	35 (79.5%)	—	<0.001

Note: Continuous variables are median [IQR]; categorical variables are n (%). The default denominators are 342 without PE and 44 with PE unless otherwise shown. Maternal age uses the analysis-safe 15–55-year field. SMD is calculated as PE minus no PE. FDR P values are Benjamini–Hochberg-adjusted Wilcoxon or categorical-test P values within their respective families. PE denotes preeclampsia; MoM, multiple of the median; PI, pulsatility index; PSV, peak systolic velocity.

Table 2. Gestational-age-specific central 95% reference intervals for bilateral mean ophthalmic artery Doppler indices

Endpoint	Week	Lower limit (90% CI)	Median (90% CI)	Upper limit (90% CI)
Mean PSV1	28	11.93 (9.38–14.37)	32.01 (31.17–32.80)	52.08 (49.49–54.72)
Mean PSV1	29	13.10 (11.27–14.77)	32.01 (31.17–32.80)	50.92 (49.04–52.86)
Mean PSV1	30	14.26 (12.70–15.76)	32.01 (31.17–32.80)	49.76 (48.26–51.23)
Mean PSV1	31	15.43 (13.69–17.10)	32.01 (31.17–32.80)	48.59 (46.98–50.15)
Mean PSV1	32	16.59 (14.28–18.83)	32.01 (31.17–32.80)	47.43 (45.32–49.47)
Mean PSV2	28	7.94 (7.22–8.69)	16.89 (16.35–17.40)	29.17 (27.97–30.25)
Mean PSV2	29	7.94 (7.22–8.69)	16.89 (16.35–17.40)	29.17 (27.97–30.25)
Mean PSV2	30	7.94 (7.22–8.69)	16.89 (16.35–17.40)	29.17 (27.97–30.25)
Mean PSV2	31	7.94 (7.22–8.69)	16.89 (16.35–17.40)	29.17 (27.97–30.25)
Mean PSV2	32	7.94 (7.22–8.69)	16.89 (16.35–17.40)	29.17 (27.97–30.25)
Mean PI	28	1.144 (1.069–1.217)	1.996 (1.942–2.047)	3.085 (2.952–3.220)
Mean PI	29	1.144 (1.069–1.217)	1.996 (1.942–2.047)	3.085 (2.952–3.220)
Mean PI	30	1.144 (1.069–1.217)	1.996 (1.942–2.047)	3.085 (2.952–3.220)
Mean PI	31	1.144 (1.069–1.217)	1.996 (1.942–2.047)	3.085 (2.952–3.220)
Mean PI	32	1.144 (1.069–1.217)	1.996 (1.942–2.047)	3.085 (2.952–3.220)
Mean peak ratio	28	37.24 (35.97–38.43)	53.65 (52.69–54.54)	77.29 (74.69–79.97)
Mean peak ratio	29	37.24 (35.97–38.43)	53.65 (52.69–54.54)	77.29 (74.69–79.97)
Mean peak ratio	30	37.24 (35.97–38.43)	53.65 (52.69–54.54)	77.29 (74.69–79.97)
Mean peak ratio	31	37.24 (35.97–38.43)	53.65 (52.69–54.54)	77.29 (74.69–79.97)
Mean peak ratio	32	37.24 (35.97–38.43)	53.65 (52.69–54.54)	77.29 (74.69–79.97)

Note: The primary reference cohort comprised 342 pregnancies that did not develop preeclampsia. Limits are the fitted 2.5th and 97.5th conditional percentiles. Confidence intervals were obtained from 1,000 participant-level bootstrap resamples. PSV1 and PSV2 denote the first and second peak systolic velocities; PI denotes pulsatility index.

Table 3. Right–left agreement of ophthalmic artery Doppler indices

Measure	n	Right mean (SD)	Left mean (SD)	Bias (95% CI)	95% limits of agreement	Lin CCC
PSV1	386	31.23 (9.79)	31.25 (9.21)	-0.02 (-0.29–0.25)	-5.29 to 5.25	0.960
PSV2	386	17.82 (5.98)	17.84 (5.96)	-0.02 (-0.07–0.03)	-0.92 to 0.88	0.997
PI	386	1.959 (0.634)	1.963 (0.626)	-0.004 (-0.011–0.004)	-0.149 to 0.142	0.993
Peak ratio	386	58.46 (15.91)	58.32 (15.71)	0.14 (-0.14–0.43)	-5.51 to 5.79	0.983

Note: Bias is right minus left. Units are cm/s for PSV1 and PSV2, unitless for PI, and percentage points for the peak ratio. CCC denotes concordance correlation coefficient.

Table 4. Bilateral mean ophthalmic artery Doppler indices and subsequent preeclampsia

Panel A. Group distributions and adjusted logistic associations

Index	No PE median [IQR]	PE median [IQR]	SMD	Group FDR P	Adjusted OR per SD (95% CI)	Model FDR P
Mean PSV1	31.75 [26.25–38.21]	24.35 [20.33–27.45]	-0.74	<0.001	0.438 (0.300–0.640)	<0.001
Mean PSV2	17.00 [14.10–20.45]	21.20 [17.69–26.80]	0.68	<0.001	1.891 (1.360–2.630)	<0.001
Mean PI	1.985 [1.790–2.250]	1.280 [0.960–1.584]	-1.16	<0.001	0.201 (0.123–0.330)	<0.001
Mean peak ratio	53.56 [48.34–60.20]	90.50 [80.50–97.86]	2.62	<0.001	8.595 (5.092–14.508)	<0.001

Panel B. Apparent single-index discrimination

Index	AUC (95% CI)	Within-sample Youden rule	Sensitivity	Specificity
Mean PSV1	0.719 (0.633–0.805)	≤27.67 cm/s	77.3%	71.6%
Mean PSV2	0.678 (0.585–0.771)	≥18.44 cm/s	75.0%	63.2%
Mean PI	0.832 (0.756–0.907)	≤1.678	88.6%	80.1%
Mean peak ratio	0.940 (0.883–0.997)	≥71.83%	93.2%	94.4%

Note: Adjusted models included gestational week at Doppler assessment, analysis-safe maternal age, and maternal BMI (n=384; 44 events). Odds ratios are per 1-SD increase. ROC thresholds maximize the Youden index in the same cohort and are exploratory. AUC denotes area under the receiver-operating-characteristic curve; OR, odds ratio; SD, standard deviation; SMD, standardized mean difference.

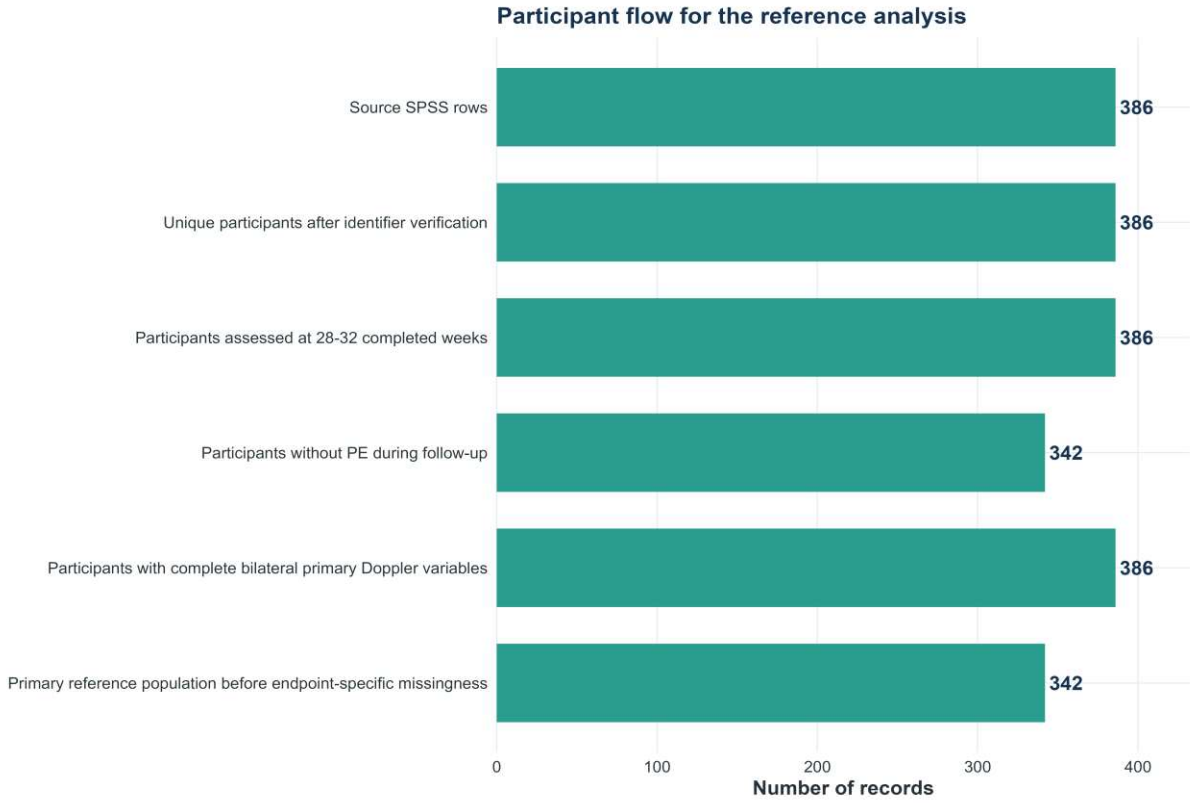


Figure 1. Participant flow for the reference analysis. The final analytical cohort comprised 386 participants; 342 pregnancies remained free of preeclampsia and formed the primary reference cohort. PE denotes preeclampsia.

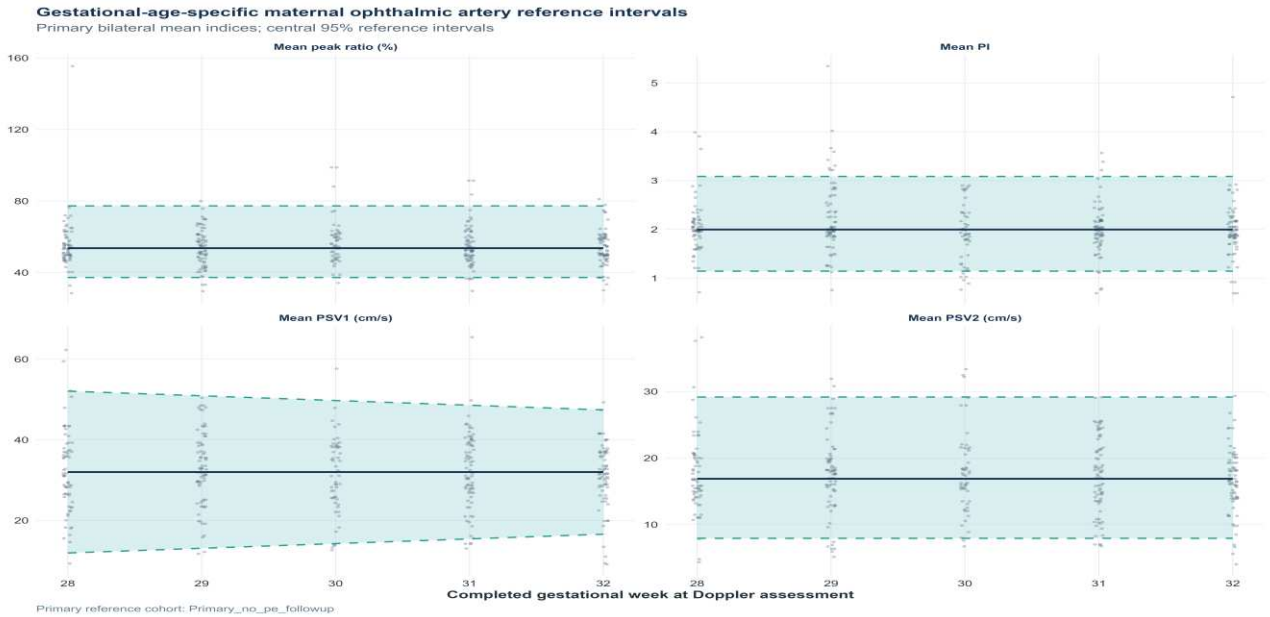


Figure 2. Gestational-age-specific central 95% reference intervals for bilateral mean ophthalmic artery Doppler indices. Points represent participants in the primary no-preeclampsia reference cohort; solid lines are fitted medians and dashed boundaries enclose the model-based central 95% reference interval. PSV1 and PSV2 denote the first and second peak systolic velocities; PI denotes pulsatility index.

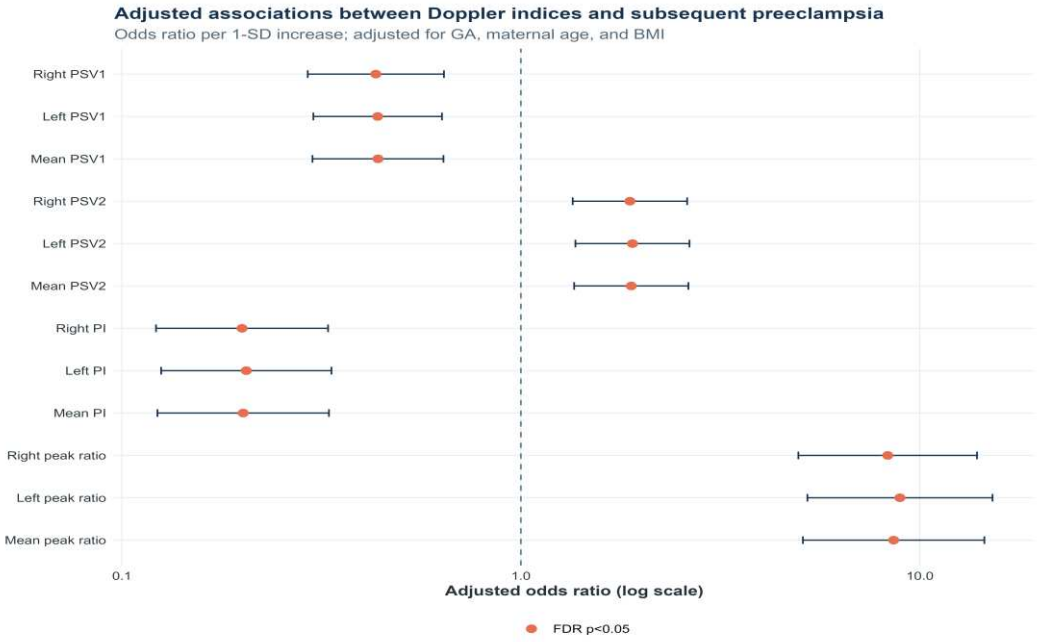

Adjusted associations between Doppler indices and subsequent preeclampsia
Odds ratio per 1-SD increase; adjusted for GA, maternal age, and BMI
Right PSV1
Left PSV1
Mean PSV1
Right PSV2
Left PSV2
Mean PSV2
Right PI
Left PI
Mean PI
Right peak ratio
Left peak ratio
Mean peak ratio
0.1
1.0
10.0
Adjusted odds ratio (log scale)
FDR p<0.05

Figure 3. Adjusted associations between ophthalmic artery Doppler indices and subsequent preeclampsia. Odds ratios and 95% confidence intervals are expressed per 1-SD increase and adjusted for gestational week at assessment, analysis-safe maternal age, and maternal body mass index. The vertical reference line denotes an odds ratio of 1.

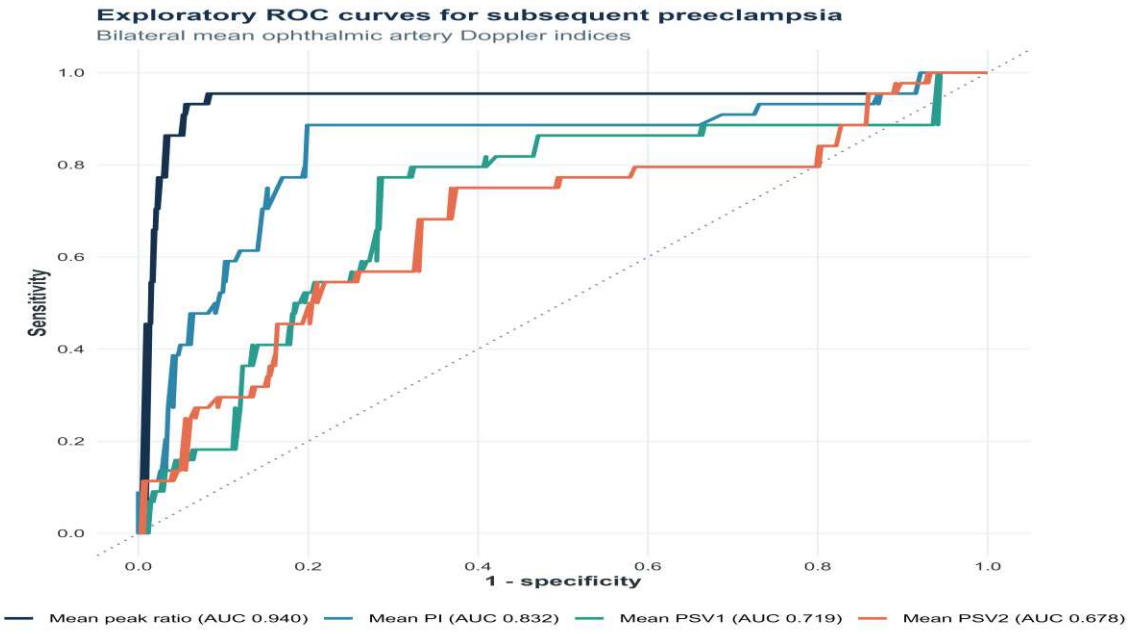


Figure 4. Exploratory receiver-operating-characteristic curves for subsequent preeclampsia. Curves show apparent single-index discrimination for four bilateral mean ophthalmic artery Doppler indices in the full cohort. Estimates were derived and evaluated in the same cohort and require independent validation.

Discussion

In this historical cohort study of 386 Iranian pregnant women, we estimated model-based reference intervals for ophthalmic artery peak systolic velocity 1 (PSV1), PSV2, pulsatility index (PI), and the PSV2/PSV1 peak ratio, calculated separately for the right eye, left eye, and binocular mean, across gestational weeks 28–32. In the reference population (342 women who remained free of preeclampsia during follow-up), the median binocular means were 32.01 cm/s for PSV1, 16.89 cm/s for PSV2, 1.996 for PI, and 53.65% for the peak ratio. Only the spread (scale) of PSV1 narrowed with advancing gestational age; the location and scale of the other three indices remained essentially stable across this five-week window. Binocular agreement was high for all four measures (Lin's concordance coefficient: 0.960–0.997; maximum mean bias: 0.144 percentage units). In an exploratory secondary analysis of the 44 preeclampsia cases (out of the full cohort), all four binocular mean indices—after adjustment for gestational age, maternal age, and BMI—were significantly associated with subsequent disease onset. The peak ratio showed the strongest association (OR = 8.595 per 1 SD; 95% CI: 5.092–14.508; apparent AUC = 0.940) and the largest standardized difference (2.62, exceeding even that of uterine artery PI at 1.89). This was followed by PI (OR = 0.201; AUC = 0.832), PSV1 (OR = 0.438; AUC = 0.719), and PSV2 (OR = 1.891; AUC = 0.678).

The concurrent but directionally divergent changes in these four indices among pregnancies that progressed to preeclampsia—decreased PSV1 and PI alongside increased PSV2 and peak ratio—point to a coherent pattern of reduced impedance in the orbito-cerebral vascular bed paired with stronger wave reflection from a drop in downstream resistance. This is consistent with prior work on maternal cerebral vascular dysautoregulation and hyperperfusion in preeclampsia (21–24). The significance of this four-way concordance extends beyond any single index reaching statistical significance: simultaneous, complementary-direction changes across all four measures lend far stronger support to a unified physiological mechanism than would independent, random fluctuations in each variable, reinforcing the construct validity of our findings (25). The rank order of apparent discriminatory power (peak ratio > PI > PSV1 > PSV2) probably reflects the fact that dimensionless, relative indices cancel out shared inter-individual measurement error between the two raw velocities (e.g., insonation angle error), sharpening the underlying physiological signal relative to absolute velocity measures (26).

Comparing our central estimates with those from international reference studies reveals a mixed picture of partial convergence and partial divergence. For the peak ratio, our median (53.65%) sits close to values reported in Chinese (54% at week 30) (1), European (mean 56%, with no age- or side-related differences) (2), and Taiwanese (mean 51% ± 10) (4) cohorts. This cross-population convergence—contrary to our initial expectation of substantial population heterogeneity—suggests the peak ratio may be relatively robust to ethnic and racial variation, at least in the second half of pregnancy. By contrast, the stability we observed at 28–32 weeks does not match Wu's gradual decline [from 0.67 at week 12 to 0.54 at week 30] (1), Diniz's weak positive correlation with gestational age across weeks 20–41 [3], or Kusuma's U-shaped pattern [declining until week 26, then rising] (5). Much of this discrepancy probably stems from differences in the gestational windows studied: our narrower 28–32 week interval probably falls on a relatively flat segment of

a broader trajectory, so our finding of local stability does not contradict the nonlinear trends reported over wider age ranges—it simply reflects our study's more limited temporal resolution.

For PI, our median of 1.996 was lower than the first-trimester mean of 2.06 reported previously (6), consistent with the well-documented decline in PI over the course of pregnancy, as also shown elsewhere (7,8). This agreement suggests our values fall along the same known physiological trajectory rather than reflecting an unexpected population deviation. Some of the remaining between-study heterogeneity is likely attributable to differing statistical approaches: unlike many prior studies that relied on simple polynomial regression or empirical percentiles within small weekly subgroups, we used a six-step location-scale approach with systematic comparison of transformations via AICc and bootstrap confidence intervals. This methodological difference probably accounts for part—though not all—of the observed numerical divergence.

From a prognostic standpoint, our findings must be interpreted against the rapidly growing body of predictive and diagnostic evidence in this field. One meta-analysis of 10,408 pregnancies showed that adding ophthalmic Doppler to maternal factors raised the AUC from 0.71 to 0.79, and to as high as 0.88 for early-onset preeclampsia (14). Another meta-analysis, of 1,425 pregnancies reported an AUC of 0.885 for the peak ratio and 0.926 for PSV2 [18]. In pivotal third-trimester screening studies, researchers showed that adding the peak ratio to maternal factors and MAP improved detection rates, particularly for imminent events, by up to 85% (20, 27, 28). Our apparent AUC of 0.940 for the peak ratio, while directionally consistent with this literature, is notably higher than these pooled estimates. This gap should be weighed against Ali's critical review, which cautioned that in small, unselected cohorts—especially when thresholds are derived and evaluated in the same sample—very high AUCs often reflect overfitting and within-sample optimization rather than true predictive accuracy in an independent population (12). Another review similarly noted wide variability in index performance across studies and a substantial risk of bias (16). Furthermore, the short median interval between Doppler assessment and clinical diagnosis in our cohort [2 days for early-onset cases, 4 days for late-onset cases, with a right-skewed distribution for the latter] suggests that our high apparent performance largely reflects temporal proximity to disease onset, rather than genuine long-range predictive capacity. This makes direct comparison with first- or second-trimester studies (23) inappropriate, and places our work conceptually closer to late-gestation screening studies than to early-prediction studies (20,21,25).

The closest comparator to our study is Saleh and colleagues, who worked in the same 28-to-32-week window in 795 participants (48 preeclampsia cases) and identified mean peak ratio, binocular PI, PAPP-A, and uterine artery PI as the most important components of a multi-marker model (29). The alignment between our findings and theirs—both in the prominence of the peak ratio and the complementary role of PI—lends meaningful external consistency to our results, though our study does not constitute an independent validation of Saleh's model. Our sample is smaller, and our statistical focus was on setting distributional references rather than building a final predictive model. Notably, our baseline characteristics also showed that pregnancies destined for preeclampsia had overt uteroplacental axis disturbances alongside the ophthalmic index changes (uterine artery PI 1.300 vs. 0.800; PAPP-A 0.55 vs. 1.15 MoM; lower fetal growth percentiles). This co-occurrence, fully consistent with Saleh's multi-marker hypothesis and related studies (20, 23, 26–28), means the true, independent added value of the ophthalmic artery peak ratio can only be judged alongside these placental markers, not in isolation. Preeclampsia is a heterogeneous disease, and no single index is

likely to capture all of its biological pathways—a combined approach remains the gold standard for any future clinical application (30).

Methodologically, this study has several strengths that strengthen the quality of evidence relative to many earlier reference studies in this area. These include a clear, pre-defined separation of the physiological reference population (342 women with no subsequent disease) from the full cohort used for outcome analysis, avoiding contamination of reference limits by subclinical phenotypes; separate modeling of location and scale with systematic comparison of three transformations based on AICc and parsimony; and 90% bootstrap confidence intervals for all limits. They also include transparent model diagnostics—including observed coverage below 95% and excess kurtosis for PI and the peak ratio, rather than presenting seemingly precise figures without an accompanying uncertainty assessment; a GAMLSS sensitivity analysis confirming the same overall conclusions under alternative distributions; complementary assessment of binocular agreement using Bland–Altman analysis and Lin's concordance coefficient instead of relying solely on correlation; and the proactive identification and correction of a systematic asymmetry in left-side peak ratio calculations (22.5% of records vs. 3.4% on the right) prior to final analysis, reflecting a high standard of data quality control (31,32).

That said, several limitations constrain the generalizability and certainty of our findings. First, the dual-center historical cohort design precluded explicit modeling of hospital- or operator-level effects. Second, the gestational age range was restricted to weeks 28–32, so our results—particularly the apparent stability of the peak ratio and PI—cannot be extrapolated to the first or early second trimester. Third, the below-nominal coverage and heavy tails observed for PI and the peak ratio indicate that these two indices, relative to PSV1 and PSV2, need further distributional validation in independent samples, and their extreme percentiles should be interpreted with added caution. Fourth, only 44 preeclampsia events occurred—including just 6 severe and 7 early-onset cases—which precluded meaningful subgroup analyses by severity or timing of onset, despite literature suggesting these subgroups may follow different hemodynamic patterns. Fifth, the reported ROC thresholds were derived and evaluated in the same dataset; without external validation, using them as clinical action thresholds would be premature. Sixth, our population was limited to Iranian women at two academic centers, so transferring these reference limits to other populations, ethnic groups, or ultrasound equipment will require separate investigation.

Practical implications

Taking these strengths and limitations together, the practical implications of this work for research and clinical practice can be summarized as follows. The reference intervals we provide offer a reliable local framework for interpreting ophthalmic artery Doppler indices in Iranian pregnancies at 28–32 weeks, and can serve as a basis for designing future validation studies and local databases. The high inter-eye agreement supports the common practice of using the binocular mean in large predictive studies, though the agreement limits show that this population-level concordance does not equate to perfect side-to-side equivalence at the individual level. The biologically meaningful and internationally consistent associations we observed for the peak ratio and PI support their potential as components of a future multi-marker model, but the primary aim of this study was to establish physiological reference values, not to build or validate a final predictive tool. Before any clinical application can be recommended, three steps remain essential: independent, preferably

multicenter, validation of thresholds and diagnostic performance in new populations; evaluation of the added value of the peak ratio and PI alongside existing combined models (MAP, uterine artery PI, PAPP-A, PlGF/sFlt-1) rather than in isolation; and reporting of calibration alongside discrimination, which was not a primary objective of the present work. Until these steps are completed, the limits presented here should be used as a research reference only, not as a tool for clinical decision-making.

Conclusion

The present findings suggest that the model-based reference intervals for maternal ophthalmic artery Doppler indices between 28 and 32 weeks' gestation—particularly for the peak ratio and PI—not only align meaningfully with internationally reported central values but also mirror the same directional relationships and rank ordering with subsequent preeclampsia described previously. This dual consistency, at both the descriptive and prognostic levels, offers compelling evidence for the construct validity of these measures in an Iranian population, and suggests that the underlying physiological patterns documented in Chinese, European, and Taiwanese cohorts are reasonably transferable to this setting.

The main contribution of this study is not the identification of a novel association per se, but rather the increased methodological rigor with which such associations are reported. Our six-step location-scale framework, the a priori separation of the reference sample from the outcome cohort, and the candid appraisal of distributional calibration limitations together form a methodological blueprint that could inform future reference-interval studies, not only in ophthalmic artery research but more broadly across obstetric and vascular diagnostics. In essence, the significance of this work should be judged on two intersecting dimensions: substantively, it reaffirms the peak ratio and PI as credible candidate biomarkers; methodologically, it offers a more disciplined and transparent approach to estimating and presenting normative limits.

Abbreviations:

OA: Ophthalmic Artery; PSV1:First Peak Systolic Velocity; PSV2:Second Peak Systolic Velocity; PR: Peak Ratio; PI: Pulsatility Index; RI: Resistance Index; GA: Gestational Age; PE: Pre-eclampsia; PAPP-A: Pregnancy-Associated Plasma Protein-A; MoM: Multiple of the Median; AICc: Small-sample Corrected Akaike Information Criterion; GAMLSS: Generalized Additive Models for Location, Scale and Shape; CCC: Concordance Correlation Coefficient; LoA: Limits of Agreement; OR: Odds Ratio; AUC: Area Under the ROC Curve; FDR: False Discovery Rate; CI: Confidence Interval

Declarations

Ethics approval and consent to participate:

Researchers confirm that all methods used in this study were carried out in accordance with relevant guidelines and regulations. This study was approved (code number: IR.ABZUMS.REC.1403.331). This study was performed in

accordance with the principles stated in the Declaration of Helsinki. Written informed consent for participation in the study was obtained from all participants at the time of ophthalmic artery Doppler assessment.

Consent for publication:

Not applicable.

Availability of data and materials:

The datasets used and analysed during the current study are available from the corresponding author on reasonable request.

Competing interests:

The authors declare that they have no competing interests

Funding:

This study funded by Alborz University of Medical Sciences.

Authors' contributions:

MA: study conception and design. ZKh and MB: Analysis and interpretation of data. MB and MY: Drafting of manuscript and Critical revision. MY, MB, MA, SES, MP, MS: Critical revision. All authors read and approved the final manuscript.

Acknowledgments:

The authors would like to thank the Clinical Research Development Unit of Emam Ali Hospital, Alborz University of Medical Sciences, Karaj, Iran, for their support, cooperation, and assistance throughout the period of study.

References:

1. Xiaojuan Wu; Dingya Cao; Xin Huang; Jieyun Chen; Nan Li; Yufang Li; Min Chen. Ophthalmic artery Doppler measurements in Chinese women with healthy pregnancies. BMC Pregnancy and Childbirth. 2026. doi: 10.1186/s12884-026-09349-x. PMID: 42363090.

2. Ladina Campana-Rüegg; Martina Hofmann; Julia Wawrla-Zepf; Ruth von Mering; Markus Gonser; Nicole Ochsenbein-Kölble; Ladina Vonzun. Ophthalmic artery Doppler: reference values in low-risk pregnant women. Archives of Gynecology and Obstetrics. 2026. doi: 10.1007/s00404-026-08489-x. PMID: 42384303.

3. Angelica Lemos Debbs Diniz; Raquel da Silva Carneiro; Alberto Borges Peixoto; Amanda Gomes Borges; Milena Fabricio Rezende; Ana Clara de Fátima da Cunha Lemes; Mariana Avelar Silveira; Isadora Souza Rufino; Edward Araujo Júnior. Reference Ranges of Maternal Ophthalmic Artery Doppler in Low-Risk Pregnancies. Journal of Ultrasound in Medicine. 2026. doi: 10.1002/jum.70110. PMID: 41211836.

4. Chi-Kang Lin; Ksenia Olisova; Merryl Esther Yuliana; Chih-Heng Chou; Kuo-Min Su; Yu-Hsuan Chen; Jui-Yu Chen; Tung-Yao Chang. The reference ranges of ophthalmic artery Doppler indices for singleton pregnancy at 20-24 weeks in Taiwan. Taiwanese Journal of Obstetrics & Gynecology. 2026. doi: 10.1016/j.tjog.2025.10.005. PMID: 41813386.

5. Raden Aditya Kusuma; Irwan Taufiqur Rachman; Althaf Setyawan; Andri Welly; Adly Nanda Al Fattah; Detty Siti Nurdiati. Reference ranges for peak systolic velocity ratio of ophthalmic artery Doppler from first to third trimester based on serial Doppler measurements. Archives of Gynecology and Obstetrics. 2025. doi: 10.1007/s00404-025-08148-7. PMID: 40879761.

6. Júlio Augusto Gurgel Alves; Bruna Yang; Paulo Cesar Praciano de Sousa; Sammya Bezerra Maia E Holanda Moura; Stefan Kane; Fabrício da Silva Costa. Reference values of maternal ophthalmic artery doppler variables in the first trimester of normal pregnancy. Journal of Clinical Ultrasound. 2014. doi: 10.1002/jcu.22122. PMID: 24691939.

7. Eloisa P Corrêa-Silva; Fernanda G Surita; Cristiane Barbieri; Sirlei S Morais; José G Cecatti. Reference values for Doppler velocimetry of the ophthalmic and central retinal arteries in low-risk pregnancy. International Journal of Gynecology & Obstetrics. 2012. doi: 10.1016/j.ijgo.2012.01.012. PMID: 22465556.

8. Cristiane Alves de Oliveira; Renato Augusto Moreira de Sá; Luis Guillermo Coca Velarde; Edson Marchiori; Hermógenes Chaves Netto; Yves Ville. Doppler velocimetry of the ophthalmic artery in normal pregnancy: reference values. Journal of Ultrasound in Medicine. 2009. doi: 10.7863/jum.2009.28.5.563. PMID: 19389894.

9. Raquel S Carneiro; Nelson Sass; Angelica L Diniz; Eder V Souza; Maria R Torloni; Antonio F Moron. Ophthalmic artery Doppler velocimetry in healthy pregnancy. International Journal of Gynecology & Obstetrics. 2008. doi: 10.1016/j.ijgo.2007.09.028. PMID: 18045602.

10. F MacKenzie; R De Vermette; C Nimrod; D Boisvert; B Jackson. Doppler sonographic studies on the ophthalmic and central retinal arteries in the gravid woman. Journal of Ultrasound in Medicine. 1995. doi: 10.7863/jum.1995.14.9.643. PMID: 7500426.

11. S Ali; D C Mukasa; D Lukakamwa; A Nakayenga; P Namagero; J Biira; J Byamugisha; A T Papageorghiou. Relationship of maternal ophthalmic artery Doppler with uterine artery Doppler, hemodynamic indices and gestational age: prospective MATERA study. Ultrasound in Obstetrics & Gynecology. 2025. doi: 10.1002/uog.29162. PMID: 39831889.

12. Shayma Ali; Zoha Mustafa; Hanna Jibran; Raaya Kooveri; Suchita D'Silva; Uwe Torsten; James Blackwell. First-trimester ophthalmic artery Doppler for prediction of early-onset and preterm preeclampsia: a systematic review and critical appraisal. BMC Pregnancy and Childbirth. 2026. doi: 10.1186/s12884-026-09618-9. PMID: 42414939.

13. Nicoleta Gana; Ancuța Năstac; Livia Mihaela Apostol; Iulia Huluță; Corina Gica; Gheorghe Peltecu; Nicolae Gica. The Role of Ophthalmic Artery Doppler in Predicting Preeclampsia: A Review of the Literature. Medicina. 2026. doi: 10.3390/medicina62010186. PMID: 41597471.

14. I Sapantzoglou; P Antsaklis; V Pergialiotis; M I Chatziioannou; Z Fasoulakis; M A Daskalaki; N Thomakos; G Daskalakis; M Theodora. Added value of ophthalmic artery Doppler in prediction of pre-eclampsia: systematic review and meta-analysis. Ultrasound in Obstetrics & Gynecology. 2025. doi: 10.1002/uog.70002. PMID: 40829118.

15. Meta Amelia; Winnee Hana Siahaan; Nicholas Wijaya; Arif Maulana Harahap; Mouza Abiyyu Rivany; Sarma Nursani Lumbanraja. Pre-eclampsia screening with maternal risk factors and ophthalmic Doppler artery: a systematic review. Hypertension in Pregnancy. 2025. doi: 10.1080/10641955.2025.2506451. PMID: 40473580.

16. Joseph Arkorful; Joyce Linda Browne; Kwame Adu-Bonsaffoh; Sam Ali; Emmanuel Srofenyoh; Kitty M W Bloemenkamp. Predictive accuracy of ophthalmic artery Doppler for pre-eclampsia: a systematic review. BMJ Open. 2025. doi: 10.1136/bmjopen-2024-094348. PMID: 40578856.

17. Xinxin Dai; Li Kang; Huiyu Ge. Doppler parameters of ophthalmic artery in women with preeclampsia: A meta-analysis. Journal of Clinical Hypertension. 2023. doi: 10.1111/jch.14611. PMID: 36495167.

18. Pollyanna F M Vaz de Melo; Leonardo Roever; Tânia M S Mendonça; Fabrício da Silva Costa; Daniel Lorber Rolnik; Angélica L D Diniz. Ophthalmic artery Doppler in the complementary diagnosis of preeclampsia: a systematic review and meta-analysis. BMC Pregnancy and Childbirth. 2023. doi: 10.1186/s12884-023-05656-9. PMID: 37173625.

19. E Kalafat; A Laoreti; A Khalil; F Da Silva Costa; B Thilaganathan. Ophthalmic artery Doppler for prediction of pre-eclampsia: systematic review and meta-analysis. Ultrasound in Obstetrics & Gynecology. 2018. doi: 10.1002/uog.19002. PMID: 29330892.

20. T Mansukhani; A Wright; A Arechvo; A Laich; M Iglesias; M Charakida; K H Nicolaides. Ophthalmic artery Doppler at 36 weeks' gestation in prediction of pre-eclampsia: validation and update of previous model. Ultrasound in Obstetrics & Gynecology. 2024. doi: 10.1002/uog.27464. PMID: 37616530.

21. Kypros H Nicolaides; Manoel Sarno; Alan Wright. Ophthalmic artery Doppler in the prediction of preeclampsia. American Journal of Obstetrics & Gynecology. 2022. doi: 10.1016/j.ajog.2020.11.039. PMID: 34292158.

22. M F Tinajero; C Faraci; M Cuenca; M Ferrer; S Paolucci; E Gratacos; F Crovetto; F Figueras. Ophthalmic artery Doppler as potential surrogate marker of angiogenic imbalance in near-term pregnancy. Ultrasound in Obstetrics & Gynecology. 2026. doi: 10.1002/uog.70270. PMID: 42366540.

23. Masayo Takata; Mikiya Nakatsuka; Takafumi Kudo. Differential blood flow in uterine, ophthalmic, and brachial arteries of preeclamptic women. Obstetrics & Gynecology. 2002. doi: 10.1016/s0029-7844(02)02244-5. PMID: 12423855.

24.M A Belfort; G R Saade; C Grunewald; G A Dildy; M A Varner; H Nisell. Effects of blood pressure on orbital and middle cerebral artery resistances in healthy pregnant women and women with preeclampsia. American Journal of Obstetrics & Gynecology. 1999. doi: 10.1016/s0002-9378(99)70261-9. PMID: 10076135.

25. Katherine G Y Lau; Allan Wright; Emmanouil Kountouris; Kypros H Nicolaides; Nikos A Kametas. Ophthalmic artery peak systolic velocity ratio distinguishes pre-eclampsia from chronic and gestational hypertension: A prospective cohort study. BJOG: An International Journal of Obstetrics & Gynaecology. 2022. doi: 10.1111/1471-0528.17061. PMID: 34913252.

26. I Sapantzoglou; A Wright; M Gallardo Arozena; R Vallenas Campos; M Charakida; K H Nicolaides. Ophthalmic artery Doppler in combination with other biomarkers in prediction of pre-eclampsia at 19-23 weeks' gestation. Ultrasound in Obstetrics & Gynecology. 2021. doi: 10.1002/uog.23528. PMID: 33142353.

27. M Sarno; A Wright; N Vieira; I Sapantzoglou; M Charakida; K H Nicolaides. Ophthalmic artery Doppler in combination with other biomarkers in prediction of pre-eclampsia at 35-37 weeks' gestation. Ultrasound in Obstetrics & Gynecology. 2021. doi: 10.1002/uog.23517. PMID: 33073902.

28. M Sarno; A Wright; N Vieira; I Sapantzoglou; M Charakida; K H Nicolaides. Ophthalmic artery Doppler in prediction of pre-eclampsia at 35-37 weeks' gestation. Ultrasound in Obstetrics & Gynecology. 2020. doi: 10.1002/uog.22184. PMID: 32857890.

29.Maasoumeh Saleh; Mahsa Naemi; Sepehr Aghajanian; Mahboubeh Saleh; Kamran Hessami; Mahmood Bakhtiyari. Diagnostic value of ophthalmic artery Doppler indices for prediction of preeclampsia at 28-32 weeks of gestation. International Journal of Gynecology & Obstetrics. 2023. doi: 10.1002/ijgo.14305. PMID: 35696254.

30. E Gibbone; I Sapantzoglou; M E Nuñez-Cerrato; A Wright; K H Nicolaides; M Charakida. Relationship between ophthalmic artery Doppler and maternal cardiovascular function. Ultrasound in Obstetrics & Gynecology. 2021. doi: 10.1002/uog.23601. PMID: 33524212.

31. Bland JM, Altman DG. Statistical methods for assessing agreement between two methods of clinical measurement. Lancet. 1986;1(8476):307–310.

32. Lin LI. A concordance correlation coefficient to evaluate reproducibility. Biometrics. 1989;45(1):255–268.

Supplementary Files

This is a list of supplementary files associated with this preprint. Click to download.

- 120stable.docx